

## Article

# Ferroptosis Inhibitory Compounds from the Deep-Sea-Derived Fungus *Penicillium* sp. MCCC 3A00126

You-Jia Hao <sup>1,2</sup>, Zheng-Biao Zou <sup>2</sup>, Ming-Min Xie <sup>2</sup>, Yong Zhang <sup>2</sup>, Lin Xu <sup>2</sup>, Hao-Yu Yu <sup>2</sup>, Hua-Bin Ma <sup>3</sup> and Xian-Wen Yang <sup>2,\*</sup> 

<sup>1</sup> College of Marine Sciences, Shanghai Ocean University, 999 Hucheng Ring Road, Shanghai 201306, China

<sup>2</sup> Key Laboratory of Marine Genetic Resources, Third Institute of Oceanography, Ministry of Natural Resources, 184 Daxue Road, Xiamen 361005, China

<sup>3</sup> Institute of Drug Discovery Technology, Ningbo University, Ningbo 315211, China

\* Correspondence: yangxianwen@tio.org.cn; Tel.: +86-592-219-5319

**Abstract:** Two new xanthenes (**1** and **2**) were isolated from the deep-sea-derived fungus *Penicillium* sp. MCCC 3A00126 along with 34 known compounds (**3–36**). The structures of the new compounds were established by spectroscopic data. The absolute configuration of **1** was validated by comparison of experimental and calculated ECD spectra. All isolated compounds were evaluated for cytotoxicity and ferroptosis inhibitory activities. Compounds **14** and **15** exerted potent cytotoxicity against CCRF-CEM cells, with IC<sub>50</sub> values of 5.5 and 3.5 μM, respectively, whereas **26**, **28**, **33**, and **34** significantly inhibited RSL3-induced ferroptosis, with EC<sub>50</sub> values of 11.6, 7.2, 11.8, and 2.2 μM, respectively.

**Keywords:** deep sea; fungus; *Penicillium* sp.; cytotoxicity; necroptosis



**Citation:** Hao, Y.-J.; Zou, Z.-B.; Xie, M.-M.; Zhang, Y.; Xu, L.; Yu, H.-Y.; Ma, H.-B.; Yang, X.-W. Ferroptosis Inhibitory Compounds from the Deep-Sea-Derived Fungus *Penicillium* sp. MCCC 3A00126. *Mar. Drugs* **2023**, *21*, 234. <https://doi.org/10.3390/md21040234>

Academic Editor: Tim Bugni

Received: 6 December 2022

Revised: 27 March 2023

Accepted: 7 April 2023

Published: 10 April 2023



**Copyright:** © 2023 by the authors. Licensee MDPI, Basel, Switzerland. This article is an open access article distributed under the terms and conditions of the Creative Commons Attribution (CC BY) license (<https://creativecommons.org/licenses/by/4.0/>).

## 1. Introduction

The oceans cover over 70% of the world's surface, with 95% of them being deeper than 1000 m. In recent years, nearly half of the new marine natural products (MNPs) have been isolated from marine microorganisms [1–3], especially fungi, the most diverse and abundant eukaryotes on Earth, which can be distributed in any currently known extreme environment [4]. As a region rarely explored, the deep sea is characterized by a high pressure, a low/high (such as hydrothermal mouth) temperature, a high salt concentration, the absence of light, oligotrophic conditions, a high halogen content, and so on. To adapt to such extreme environments, deep-sea-derived microorganisms must develop special metabolic mechanisms, giving rise to tremendous secondary metabolites with unique structures and potent bioactivities [5]. For more than half a century, MNPs have been continuously discovered, but those from the deep sea are rare [6,7]. In recent years, with the development of deep-sea sample collection technology, reports of deep-sea MNPs have increased significantly. As an important group of deep-sea microorganisms, fungi can produce a large number of structurally novel and biologically active secondary metabolites, which have attracted extensive attention from researchers. For example, vercytochalasins A and B are two novel, biosynthetically related cytochalasins isolated from *Curvularia verruculosa*, the endophytic fungus of the deep-sea lobster *Shinkaia crosnieri*. Vercytochalasin A is the most potent natural product against angiotensin-I-converting enzyme (ACE), with an IC<sub>50</sub> value of 505 nM [8]. Chevalinulins A and B are two indole alkaloids with a rare spiro-[bicyclo[2.2.2]octane-diketopiperazine] skeleton. They both exhibit significant in vivo proangiogenic activity in transgenic zebrafish [9].

Xanthenes, also known as 9H-xanthen-9-ones, are a class of yellow compounds bearing a dibenzo-γ-pyrone scaffold. They are widely distributed in plants, lichens, and microorganisms of terrestrial and marine origin, and exhibit diverse biological activities such as antiviral [10], cytotoxic [11], antibacterial [12], antifungal [13], and hypoglycemic [14] activities. The molecular skeleton of xanthenes can bind with a variety of targets, so this

family of compounds is often called “privileged structures” [15]. They are regarded as typical aromatic polyketone and appear in the form of fully aromatic or hydrogenated derivatives [16]. In general, xanthenes can be classified into monomers, dimers, and heterodimers. According to the degree of hydrogenation of the skeleton aromatic ring, they can be further split into four subclasses: fully aromatic xanthenes, dihydro-, tetrahydro-, and hexahydro-xanthenes [16]. From 2010 to 2021, 100 marine xanthenes were reported, among which 51 were new compounds. Most of the new xanthenes were derived from marine fungi, especially deep-sea fungi isolated from deep-sea sediments or organisms [17]. Therefore, deep-sea-derived fungi are undoubtedly an important resource for the discovery of xanthenes with novel structures and significant bioactivities.

During our ongoing search for bioactive secondary metabolites from deep-sea-derived fungi [18–21], the crude extract of *Penicillium* sp. MCCC 3A00126 isolated from the Eastern Pacific Ocean at a depth of 5246 m showed significant cytotoxicity against acute lymphoblastic leukemia CCRF-CEM with the cell survival rate of 29.8 % under the concentration of 10  $\mu\text{g}/\text{mL}$ . Therefore, it was subjected to a systematic chemical investigation. As a result, two novel (**1** and **2**) and 13 known (**3–15**) xanthenes were isolated and purified, along with 21 known miscellaneous compounds (**16–36**) (Figure 1). Herein, the details of isolation, structure, and bioactivity are reported.

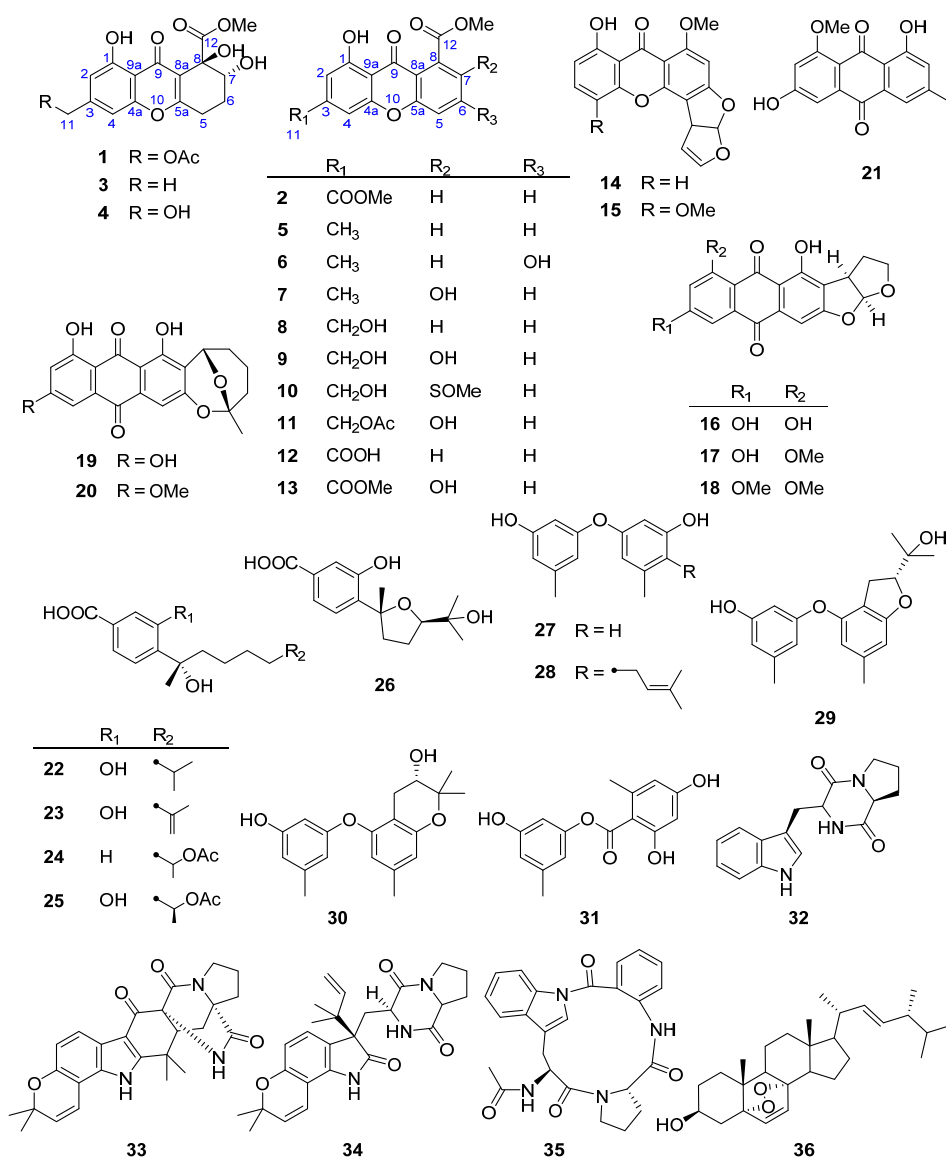


Figure 1. Chemical structures of compounds 1–36 isolated from *Penicillium* sp. MCCC 3A00126.

## 2. Results and Discussion

Compound **1** was obtained as a colorless gum. The molecular formula  $C_{18}H_{18}O_9$  was determined by the positive HR-ESI-MS (high resolution electrospray mass spectrometry spectrum) at  $m/z$  401.0839  $[M + Na]^+$ , suggesting ten degrees of unsaturation. The  $^1H$  (Figure S1 in the Supplementary Materials) and  $^{13}C$  (Figure S2 in the Supplementary Materials) NMR (nuclear magnetic resonance) spectroscopic data (Table 1) exhibited the presence of one methoxyl [ $\delta_H$  3.84 (3H, s);  $\delta_C$  53.4 q], one methyl singlet [ $\delta_H$  2.16 (3H, s);  $\delta_C$  20.8 q], one oxygenated [ $\delta_H$  5.13 (2H, s);  $\delta_C$  65.0 t], and two aliphatic [ $\delta_H$  2.25 (2H, m), 2.87 (2H, m);  $\delta_C$  24.2 t, 26.1 t] methylene groups, one oxygenated aliphatic [ $\delta_H$  4.09 (1H, dd,  $J = 10.3, 3.6$  Hz);  $\delta_C$  72.6 d] and two olefinic [ $\delta_H$  6.75 (1H, s), 6.86 (1H, s);  $\delta_C$  109.9 d, 105.5 d] methines, as well as ten quaternary carbons including one oxygenated aliphatic ( $\delta_C$  76.2 s), six olefinic ( $\delta_C$  109.6 s, 117.0 s, 145.0 s, 156.1 s, 160.7 s, 167.4 s), and three carbonyl ( $\delta_C$  170.5 s, 172.7 s, 182.0 s) carbons. These signals were very similar to aspergillusone B (**4**) [22], except for an additional acetyl group [ $\delta_H$  2.16 (3H, s);  $\delta_C$  20.8 q, 170.5 s] at the C-11 position. This was supported by the downfield shifts of H-11 from  $\delta_H$  4.76 to  $\delta_H$  5.13 and C-11 from  $\delta_C$  64.4 to  $\delta_C$  65.0. Further confirmation was obtained by the HMBC (heteronuclear multiple-bond correlation) correlations of H<sub>2</sub>-11 to the carbonyl group of the acetyl moiety; and the  $^1H$ - $^1H$  COSY (correlation spectroscopy) cross peaks of H<sub>2</sub>-6 to H<sub>2</sub>-5/H-7 (Figure 2).

**Table 1.**  $^1H$  (400 MHz) and  $^{13}C$  (100 MHz) NMR data of **1** and **2** in  $CDCl_3$  ( $\delta$  in ppm,  $J$  in Hz within parenthesis).

No.	<b>1</b>		<b>2</b>	
	$\delta_C$	$\delta_H$	$\delta_C$	$\delta_H$
1	160.7 C		161.7 C	
2	109.9 CH	6.75 s	111.6 CH	7.44 s
3	145.0 C		137.6 C	
4	105.5 CH	6.86 s	108.1 CH	7.60 s
4a	156.1 C		155.4 C	
5	26.1 CH <sub>2</sub>	2.87 m	119.6 CH	7.59 (d, 8.0)
6	24.2 CH <sub>2</sub>	2.25 m	135.5 CH	7.81 (dd, 8.0, 7.2)
7	72.6 CH	4.09 (dd, 10.3, 3.6)	123.1 CH	7.36 (d, 7.2)
8	76.2 C		133.7 C	
8a	117.0 C		117.4 C	
9	182.0 C		180.9 C	
9a	109.6 C		111.0 C	
10	167.4 C		156.2 C	
11	65.0 CH <sub>2</sub>	5.13 s	165.3 C	
12	172.7 C		169.2 C	
11-OMe			52.8 CH <sub>3</sub>	3.98 s
11-OAc	170.5 C			
	20.8 CH <sub>3</sub>	2.16 s		
12-OMe	53.4 CH <sub>3</sub>	3.84 s	53.2 CH <sub>3</sub>	4.04 s
1-OH		11.99 s		12.20 s

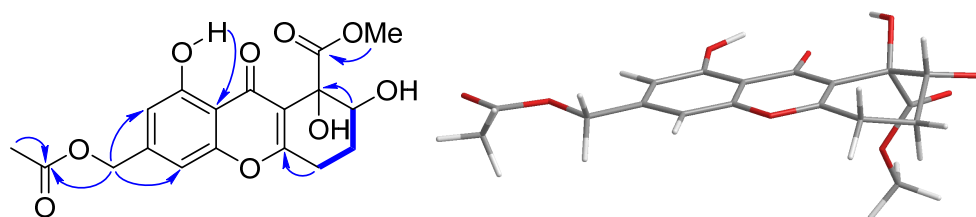


**Figure 2.** Key  $^1H$ - $^1H$  COSY and HMBC correlations and MM2 model of the most stable conformer in the 7,8-anti diol found in **1**.

The coupling constants between H-7 and H<sub>2</sub>-6 of **1** ( $J = 10.3$  Hz,  $3.6$  Hz) indicated the same pseudoaxial position of H-7 as that of **4** [22], as it was found in a simple MM2

conformational study of both possible 7,8-anti and 7,8-syn diols (Figure 2). The observed optical rotation value of **1** ( $[\alpha]_D^{25} -82.5$ ) was close to that of **4** ( $[\alpha]_D^{25} -46.3$ ) in the same concentration ( $c$  0.2) and the same solvent ( $\text{CHCl}_3$ ), ( $c$  0.2,  $\text{CHCl}_3$ ), suggesting they have the same absolute configuration at C-7 and C-8. For the further confirmation, the ECD (electron circular dichroism) spectra were calculated for (7*R*,8*R*)-**1** (**1a**) and its enantiomer (7*S*,8*S*)-**1** (**1b**) using Yinfo Cloud Computing Platform (<https://cloud.yinfotek.com>, accessed on 13 June 2022). Thirty states of each seven conformers were calculated to generate the ECD curves. As shown in Figure 3, the calculated ECD spectrum of **1a** was consistent with that of the experimental one. On the basis of the above evidence, compound **1** was then elucidated as 11-*O*-acetylaspergillusone B.

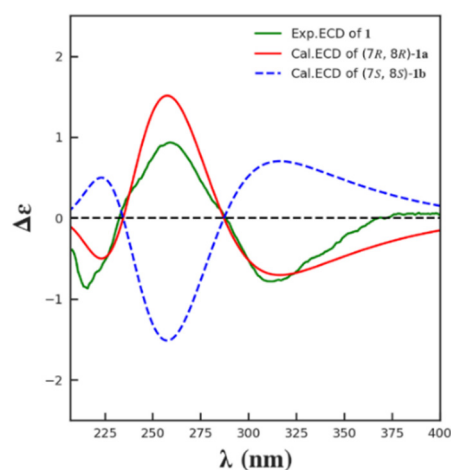


Figure 3. Calculated and experimental ECD spectra of **1**.

Compound **2** was obtained as a amorphous yellow solid. The molecular formula  $\text{C}_{17}\text{H}_{12}\text{O}_7$  was established by its positive HR-ESI-MS spectrum at  $m/z$  351.0482  $[\text{M} + \text{Na}]^+$ . The  $^1\text{H}$  and  $^{13}\text{C}$  data of **2** showed the presence of two methoxyls, five methines and ten quaternary carbons, which were closely related to those of huperxanthone A (**13**) [14], except that the  $sp^2$  quaternary carbon at C-7 ( $\delta_{\text{C}}$  151.1 s) in **13** was changed as an  $sp^2$  methine ( $\delta_{\text{C}}$  123.1 d) in **2**. By detailed analysis of its HSQC (heteronuclear single quantum correlation),  $^1\text{H}$ - $^1\text{H}$  COSY, HMBC, and NOESY (nuclear Overhauser effect) spectroscopic data, compound **2** was then established as 7-dehydroxyhuperxanthone A.

By comparison of the NMR and MS data with those published in the literature, 34 known compounds were identified as 13 xanthenes: (7*R*,8*R*)- $\alpha$ -diversonolic ester (**3**) [23,24], aspergillusone B (**4**) [22], 8-hydroxy-6-methyl-9-oxo-9H-xanthene-1-carboxylate (**5**) [25], yicathin B (**6**) [26], pinselin (**7**) [27], sydowinins A (**8**) and B (**9**) [28], huperxanthone C (**10**) [14], 13-*O*-acetylsydowinin B (**11**) [29], 8-(methoxycarbonyl)-1-hydroxy-9-oxo-9H-xanthene-3-carboxylic acid (**12**) [25], huperxanthone A (**13**) [14], sterigmatocystin (**14**) [30], 5-methoxysterigmatocystin (**15**) [31]; six anthraquinones: versicolorin B (**16**) [32], 8-*O*-methylversicolorin B (**17**) [33], anthraquinone aversin (**18**) [34], averufin (**19**) [35], 6-*O*-methylaverufin (**20**) [36], questin (**21**) [37]; five sesquiterpenoids: (*S*)-(+)-sydonic acid (**22**) [38], (*S*)-(+)-11-dehydroxydonic acid (**23**) [38], (−)-12-acetoxy-1-deoxysydonic acid (**24**) [39], (7*S*,11*S*)-(+)-12-acetoxydonic acid (**25**) [38], (−)-(7*R*,10*R*)-*iso*-10-hydroxydonic acid (**26**) [39]; four diphenyl ethers: diorcinol (**27**) [40], verticilatin (**28**) [41], (*R*)-3-((2-(2-hydroxypropan-2-yl)-6-methyl-2,3-dihydrobenzofuran-4-yl)oxy)-5-methylphenol (**29**) [42], (3*S*)-3,4-dihydro-5-(3-hydroxy-5-methylphenoxy)-2,2,7-trimethyl-2*H*-chromen-3-ol (**30**) [43]; one polyketone: 3-hydroxy-5-methylphenyl-2,4-dihydroxy-6-methylbenzoate (**31**) [44]; four indole alkaloids: brevianamide F (**32**) [45], notoamide I (**33**) [46], notoamide C (**34**) [47], psychrophilin D (**35**) [48], and one steroid: 5*a*,8*a*-epidioxy-22*E*-ergosta-6,9(11)-trien-3 $\beta$ -ol (**36**) [49].

Since the crude extract of *Penicillium* sp. MCCC 3A00126 showed a potent anti-proliferative effect on CCRF-CEM, all 36 isolates were subjected to cytotoxicity tests on the same acute lymphoblastic leukemia using the CCK-8 assay. As shown in Figure 4, under a concentration of 20  $\mu$ M, two compounds, **14** and **15**, exerted potent activity, with cell survival rates of 6.2% and 7.3%, respectively, while seven compounds, **4**, **8**, **11**, **17**, **20**, **28**, and **29**, showed weak effects, with cell survival rates of 70.2%, 78.5%, 78.8%, 62.3%, 75.8%, 55.3%, and 55.3%, respectively. Interestingly, compounds **14** and **15** possess a difuran ring at C-5 and C-6, which might be the key to the bioactivity.

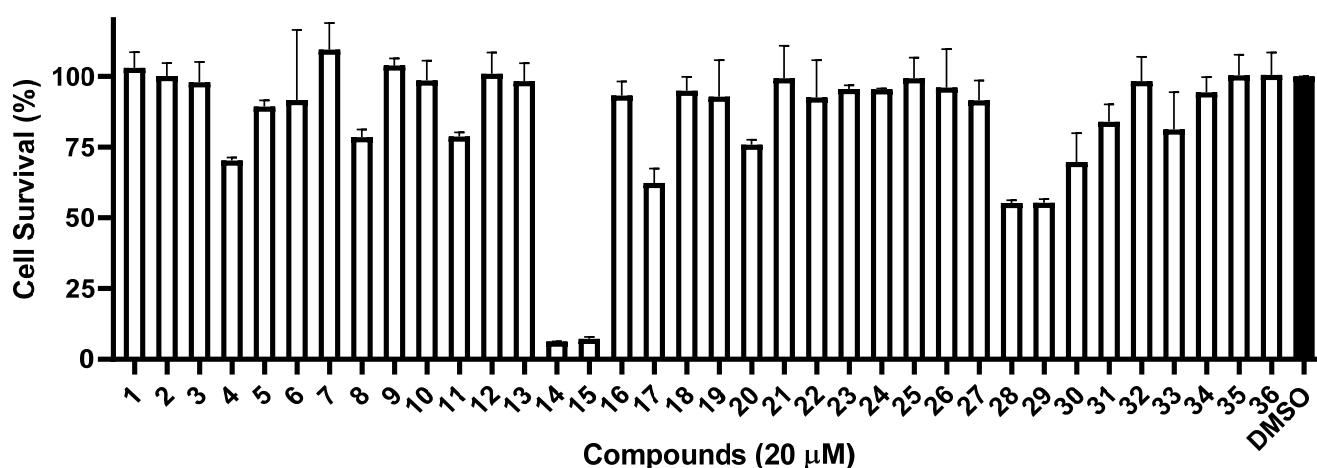


Figure 4. Cytotoxicity of compounds 1–36 against CCRF-CEM cells.

Compounds **14** and **15** were further evaluated to determine their 50% inhibiting concentration ( $IC_{50}$ ) against CCRF-CEM using five different concentrations: 1  $\mu$ M, 2.5  $\mu$ M, 5.0  $\mu$ M, 10.0  $\mu$ M, and 20.0  $\mu$ M. The  $IC_{50}$  values of **14** and **15** were found to be 5.5  $\mu$ M and 3.5  $\mu$ M, respectively (Figure 5).

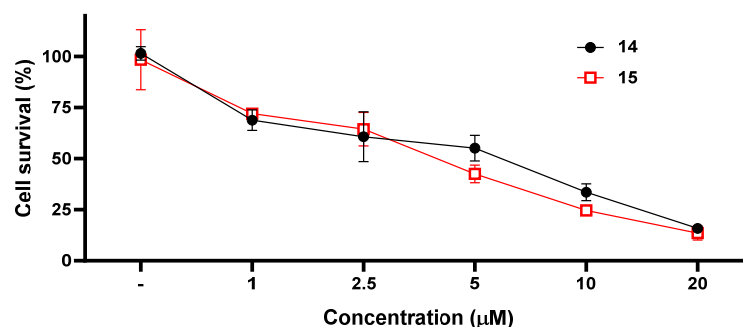


Figure 5.  $IC_{50}$  values of compounds **14** and **15** against CCRF-CEM cells.

Ferroptosis is an iron-dependent mode of necroptosis induced by certain small molecules, such as RSL3 (the glutathione peroxidase 4 inhibitor), which is different from apoptosis, necrolysis, and autophagy [50]. Its main characteristics are the generation of ROS (reactive oxygen species), LPO (lipid peroxidation), and iron accumulation. RSL3 acts on specific targets in cells and causes a reduction in antioxidants GSH (glutathione) and GPX4 (glutathione peroxidase 4), resulting in the accumulation of ROS in cells, LPO in cells, and ferroptosis in cells under the synergistic effect of iron [51]. Many tumor cells that are easy to metastasize are prone to ferroptosis, so inducing and inhibiting ferroptosis for pharmacological regulation has great potential in the treatment of certain cancers.

To further investigate whether these isolates could inhibit ferroptosis, RSL3, the GPX4 inhibitor, was used to induce ferroptosis in CCRF-CEM cells. As a result, compounds **26**, **28**, **33**, and **34** exerted strong inhibition, with cell survival rates of 83.9%, 110.0%, 99.0%, and 105.2%, respectively, under a concentration of 20  $\mu$ M. Additionally, compounds **3**, **27**,

29, and 30 showed weak activity, with cell survival rates of 36.0%, 16.6%, 19.5%, and 28.8%, respectively (Figure 6).

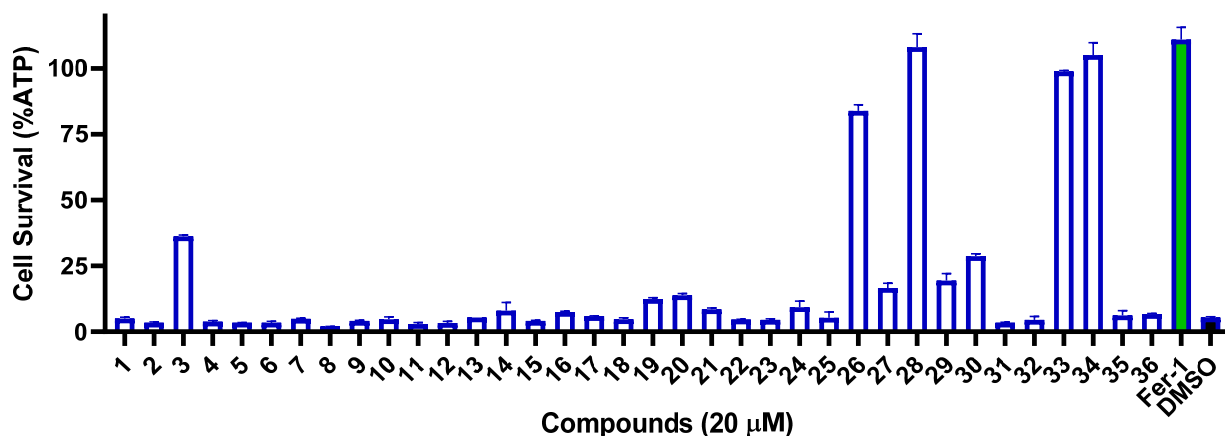


Figure 6. Inhibitory effects of compounds 1–36 on RSL3-induced ferroptosis in CCRF-CEM cells.

To determine the 50% effective concentration (EC<sub>50</sub>) of compounds 26, 28, 33, and 34, four different concentrations (1 μM, 5.0 μM, 10.0 μM, and 20.0 μM) were adopted on RSL3-induced ferroptosis in CCRF-CEM cells, providing corresponding IC<sub>50</sub> values of 11.6 μM, 7.2 μM, 11.8 μM, and 2.2 μM, respectively (Figure 7).

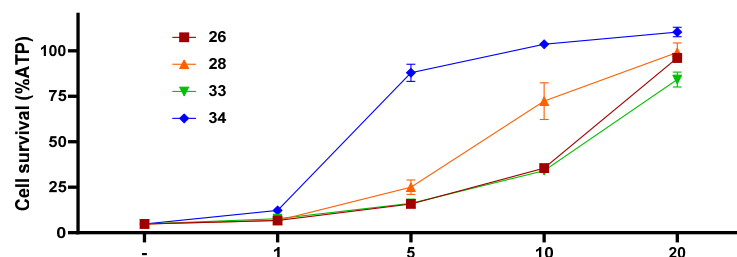


Figure 7. EC<sub>50</sub> values of compounds 26, 28, 33, and 34 on RSL3-induced ferroptosis in CCRF-CEM cells.

As ferroptosis was triggered by lipid peroxidation, many ferroptosis inhibitors exhibited antioxidant activity, such as ferrostatin-1 (Fer-1) [50,52,53]. Therefore, the 2,2-diphenyl-1-picrylhydrazyl (DPPH) assay was performed on these compounds to evaluate their intrinsic antioxidant potential. However, none showed positive effects under a concentration of 20 μM (Figure 8), indicating that compounds 26, 28, 33, and 34 might exert ferroptosis inhibition by other mechanisms instead of DPPH.

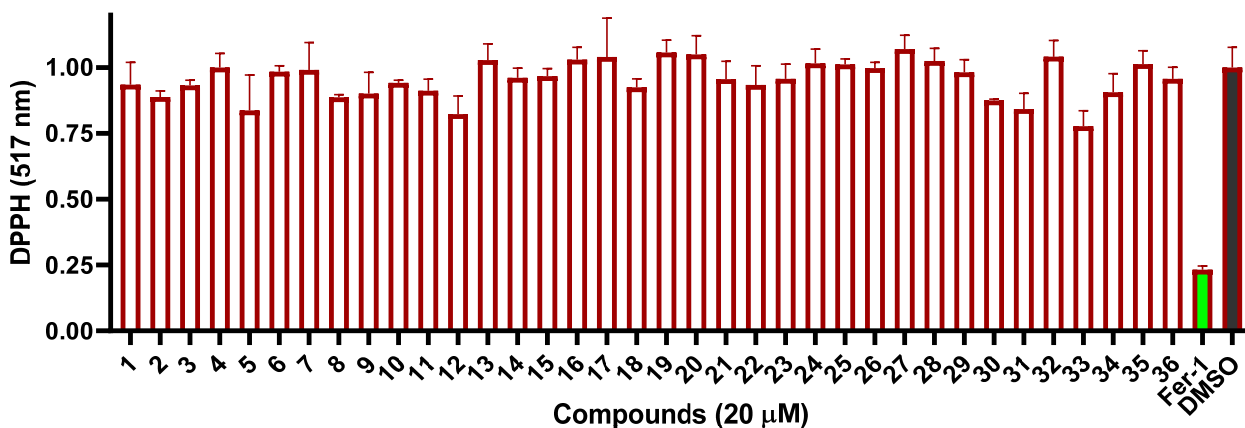


Figure 8. DPPH radical scavenging activities of compounds 1–36.

### 3. Materials and Methods

#### 3.1. General Experimental Procedures

The HR-ESI-MS spectra were obtained on a Waters Xevo G2 Q-TOF mass spectrometer equipped with a Spray™ ESI source in both the positive and negative ion mode. NMR spectra were recorded in CDCl<sub>3</sub>, CD<sub>3</sub>OD, or DMSO-*d*<sub>6</sub> on a Bruker Avance III 400 Mz spectrometer at room temperature. Optical rotation was measured by an Anton Paar MCP 100 polarimeter. UV and ECD spectra were acquired on a JASCO J-810 spectropolarimeter. Preparative HPLC (high-performance liquid chromatography) separations for purification were carried out on an Agilent 1260 system with a semi-preparative chromatographic column (COSMOSIL 5C<sub>18</sub>-MS-II, 5PFP, SL-II, 250 mm × 10 mm). Materials for column chromatography (CC) included silica gel, ODS (octadecylsilyl), and Sephadex LH-20.

#### 3.2. Biological Material

The deep-sea-derived fungus *Penicillium* sp. MCCC 3A00126 was isolated from a sediment sample collected from the Eastern Pacific Ocean at a depth of 5246 m by Professor De-Zan Ye of the Third Institute of Oceanography, Ministry of Natural Resources, in September 2003. The 18S rRNA gene sequence alignment (AM18217) showed great similarity (99.88%) to *Penicillium* sp. PB g (GenBank accession number MK372218.1); therefore, it was identified to be *Penicillium* sp. It was deposited at the Marine Culture Collection of China (Xiamen, China) with accession number MCCC 3A00126.

#### 3.3. Fermentation, Isolation, and Purification

The strains stored at −80 °C were inoculated into a 250 mL conical flask containing 100 mL PDB culture medium to conduct initial activation for three days in a shaking table culture at 28 °C. Then, under the same culture conditions, 1 mL of the fungal liquid was placed in another 1 L conical flask containing 250 mL of PDB medium to conduct secondary activation.

The secondary activated fungal strain was inoculated into 60 Erlenmeyer flasks containing 80 g rice and 120 mL distilled water. The fermentation was kept under static conditions at 25 °C. After 40 days, 400 mL of EtOAc was added to each flask over 12 h. The organic solvent was filtered. The procedure was repeated four times. The organic solvents were combined and concentrated to a small volume. The latter was dissolved in MeOH and extracted by PE (petroleum ether) three times. The MeOH layer was concentrated to provide a crude extract (26.3 g), which was subjected to MPLC (medium-pressure liquid chromatography) over silica gel using the CH<sub>2</sub>Cl<sub>2</sub>/MeOH gradient (100% → 70%) to obtain four fractions (Fr.1–Fr. 4). Fraction Fr.1 (0.46 g) was separated by repeated column chromatography (CC) over ODS (MeOH/H<sub>2</sub>O) and Sephadex LH-20 (CH<sub>2</sub>Cl<sub>2</sub>/MeOH, 1:1 and 0:1), then purified by semi-prep. HPLC (C18, 10 × 250 mm, MeOH/H<sub>2</sub>O, 80% → 100%), providing **2** (15.0 mg) and **5** (14.0 mg). Fraction Fr.2 (1.1 g) was subjected to CC over ODS and Sephadex LH-20, then purified by semi-prep. HPLC (C18, 10 × 250 mm, MeOH/H<sub>2</sub>O, 70% → 90%), yielding **14** (2.0 mg), **15** (3.0 mg), and **18** (5.4 mg). Fraction Fr.3 (3.7 g) was separated by ODS CC with MeOH/H<sub>2</sub>O (30% → 80%, 3 h, 80% → 90%, 3 h) to obtain thirteen subfractions (Fr.3.1–Fr.3.13). Subfractions (Fr.3.1–Fr.3.9) were subjected to CC over Sephadex LX-20 using MeOH to yield compounds **3** (2.0 mg), **10** (9.0 mg), **11** (4.0 mg), **13** (8.0 mg), **16** (2.0 mg), **19** (2.5 mg), **20** (6.0 mg), **28** (9.5 mg), and **36** (28.0 mg), respectively. Sub-fraction Fr.3.10 was subjected to CC over Sephadex LH-20 (CH<sub>2</sub>Cl<sub>2</sub>/MeOH, 1:1) and silica gel (CH<sub>2</sub>Cl<sub>2</sub>/MeOH, 45:1), followed by separation using HPLC (C18, 10 mm × 250 mm, MeOH/H<sub>2</sub>O, 80% → 90%) to give **8** (15.0 mg) and **9** (2.0 mg). Fr.3.11 was separated by CC over LH-20 (MeOH) and silica gel (CH<sub>2</sub>Cl<sub>2</sub>/MeOH, 55:1) to obtain **12** (1.0 mg). Fr.3.12 was purified by semi-prep. HPLC (PFP-pentafluorophenyl group, 10 mm × 250 mm, MeOH/H<sub>2</sub>O, 60% → 90%), yielding **21** (3.0 mg), **29** (6.6 mg), and **30** (1.3 mg). Fr.3.13 was further separated by HPLC (C18, 10 mm × 250 mm, MeOH/H<sub>2</sub>O, 55% → 85%) to yield **6** (3.0 mg).

Using similar procedures, fraction Fr.4 (3.3 g) was separated into thirteen subfractions (Fr.4.1–Fr. 4.13) by CC over ODS (MeOH/H<sub>2</sub>O, 5 → 60%, 4 h, 60% → 100%, 2 h). Compounds **1** (8.0 mg), **4** (23.3 mg), **17** (23.0 mg), **22** (39.0 mg), **27** (7.0 mg), and **31** (19.8 mg) were obtained from Fr.4.1–Fr.4.6 by CC over Sephadex LH-20 (MeOH). Fr.4.7 and Fr.4.8 were separated by HPLC (C18, 10 mm × 250 mm, MeOH/H<sub>2</sub>O, 35% → 65%) to obtain **26** (1.0 mg) and **32** (2.6 mg), respectively. Fr.4.9 was subjected to Sephadex LH-20 CC, eluting with MeOH, and then purification by HPLC (C18, 10 mm × 250 mm, MeOH/H<sub>2</sub>O, 55% → 85%) afforded **24** (3.0 mg) and **25** (9.5 mg). Fr.4.10 was separated by HPLC on silica gel (10 mm × 250 mm, CH<sub>2</sub>Cl<sub>2</sub>/MeOH, 100% → 90%) to yield **35** (12.0 mg). Compounds **23** (2.5 mg) and **33** (1.7 mg) were also separated from Fr.4.11 using HPLC (C18, 10 mm × 250 mm, MeOH/H<sub>2</sub>O, 60% → 80%). Fr.4.12 was chromatographed by CC over silica gel (PE/EtOAc, 3:1) to yield **7** (3.2 mg) and Fr.4.13 was subjected HPLC (C18, 10 mm × 250 mm, MeOH/H<sub>2</sub>O, 55% → 85%) to yield **34** (0.7 mg).

11-*O*-Acetylaspergillusone B (**1**). Colorless gum;  $[\alpha]_D^{25}$  −82.5 (*c* 0.2, CHCl<sub>3</sub>), −19.0 (*c* 0.1, MeOH); UV (2.6 mM, MeOH)  $\lambda_{\max}$  (log  $\epsilon$ ) 212 (2.32), 240 (2.42), 289 (1.69), 331 (2.04) nm; ECD (2.6 mM, MeOH)  $\lambda_{\max}$  ( $\Delta\epsilon$ ) 216 (1.99), 263 (2.06), 313 (1.79); <sup>1</sup>H and <sup>13</sup>C NMR data, Table 1; HRESIMS *m/z* 401.0839 [M + Na]<sup>+</sup> (calcd for C<sub>18</sub>H<sub>18</sub>O<sub>9</sub>Na, 401.0849).

7-Dehydroxyhyperxanthone A (**2**). Yellow amorphous solid; UV (3.0 mM, MeOH)  $\lambda_{\max}$  (log  $\epsilon$ ) 266 (3.23); <sup>1</sup>H and <sup>13</sup>C NMR data, Table 1; HRESIMS *m/z* 351.0482 [M + Na]<sup>+</sup> (calcd for C<sub>17</sub>H<sub>12</sub>O<sub>7</sub>Na, 351.0481).

### 3.4. ECD Calculation

ECD calculations were performed using Yinfo Cloud Computing Platform, a user-friendly and versatile web server for biomedical, material, and statistical research (<https://cloud.yinfotek.com>, accessed on 13 June 2022). The conformational analysis of compound **1** was carried out using the MMFF94 force field at an energy cutoff of 7.0 kcal/mol and an RMSD threshold of 0.5 Å. A total of thirteen conformations were obtained from the conformational analysis, and seven of which, accounting for more than 1%, were selected for further screening. The seven conformers were relocated and confirmed at the PM6, HF/6-31G(d), and B3LYP/6-1G(d) level to obtain three dominant conformers. Further, the calculation of the theoretical ECD spectra at the B3LYP/6-311G(d, p) level was conducted in MeOH. The final spectrum was obtained by averaging each conformer using the Boltzmann distribution.

### 3.5. Cytotoxic Experiment

CCRF-CEM cells (CL-0058), kindly provided by Procell Life Science & Technology Co., Ltd. (Wuhan, China), were cultured in RPMI-1640 at 37 °C in a humidified atmosphere containing 5% CO<sub>2</sub> with 10% inactive fetal bovine serum, 2 mM L-glutamine, 100 IU penicillin, and 100 mg/mL streptomycin. The cytotoxicity experiment was conducted using the CCK-8 (Cell Counting Kit-8) assay. Briefly, 4000 cells were seeded on a 96-well plate. After 24 h, different concentrations of the tested compounds were added, and the incubation continued for 48 h. The CCK-8 assay was performed with MD Spectra Max Paradigm.

### 3.6. Ferroptosis Inhibitory Assay

As previously reported [54], 10,000 CCRF-CEM cells were seeded on a 96-well plate for 24 h. Then, ferrostatin-1 (1 μM, as the positive control) and different concentrations of the tested compounds, ranging from 1 μM to 20 μM, were added for first-round screening. After 0.5 h, RSL3 (2 μM) was added to trigger ferroptosis. Four hours later, cellular ATP was detected using the Cell Titer Glo Luminescent Cell Viability assay kit (G7570, Promega, Madison, WI, USA) according to the manufacturer's instructions. Then, the EC<sub>50</sub> values were determined as the indicated concentration.

### 3.7. DPPH Assay

According to a reported procedure [55], the stable radical DPPH (2,2-diphenyl-1-picrylhydrazyl) was dissolved in MeOH to a final working concentration of 100  $\mu$ M. Then, 1  $\mu$ L of the indicated compounds dissolved in DMSO (10 mM) was added to a final concentration of 100  $\mu$ M, inverted several times, and allowed to incubate at room temperature for 30 minutes. Samples were then aliquoted to a 96-well microplate and absorbance at 517 nm was recorded using Spectra Max Paradigm (Molecular Devices, San Jose, CA, USA). The relative DPPH normalized to the background (MeOH only) showed the mean  $\pm$  SD, and the experiments were triplicated.

## 4. Conclusions

Systematic chemical investigation of the deep-sea fungus *Penicillium* sp. 3A00126 yielded 36 compounds, comprising fifteen xanthenes (3–15), six anthraquinones (16–21), five sesquiterpenoids (22–26), four diphenyl ethers (27–30), one polyketone (31), four indole alkaloids (32–35), and one steroid (36). Compound 1, named 11-*O*-acetylaspergillusone B, is a new tetrahydroxanthone, and compound 2, 7-dehydroxyhyperxanthone A, is a new, fully aromatic xanthone. All 36 isolates were tested for cytotoxicity and ferroptosis inhibitory effects. Sterigmatocystin (14) and 5-methoxysterigmatocystin (15) showed potent cytotoxicity against CCRF-CEM cells, with IC<sub>50</sub> values of 5.5  $\mu$ M and 3.5  $\mu$ M, respectively, whereas (–)-(7*R*,10*R*)-*iso*-10-hydroxysydowic acid (26), verticilatin (28), notoamide I (33), and notoamide C (34) significantly inhibited RSL3-induced ferroptosis, with EC<sub>50</sub> values of 11.6  $\mu$ M, 7.2  $\mu$ M, 11.8  $\mu$ M, and 2.2  $\mu$ M, respectively.

**Supplementary Materials:** The following are available online at <https://www.mdpi.com/article/10.3390/md21040234/s1>, Figures S1–S13: One-dimensional and two-dimensional NMR and HR-ESI-MS spectra of compound 1 and 2.

**Author Contributions:** X.-W.Y. designed the project; Y.-J.H. and Z.-B.Z. isolated and purified compounds. L.X., M.-M.X. and Y.Z. performed the fermentation. H.-B.M. conducted the biological experiments. Y.-J.H., H.-Y.Y. and X.-W.Y. analyzed the data and wrote the paper, while critical revision of the publication was performed by all authors. All authors have read and agreed to the published version of the manuscript.

**Funding:** The work was financially supported by Xiamen Southern Oceanographic Center Project (22GY007HJ07) and the National Natural Science Foundation of China (22177143).

**Institutional Review Board Statement:** Not applicable.

**Informed Consent Statement:** Not applicable.

**Data Availability Statement:** Not applicable.

**Conflicts of Interest:** The authors declare no conflict of interest.

## References

1. Carroll, A.R.; Copp, B.R.; Davis, R.A.; Keyzers, R.A.; Prinsep, M.R. Marine natural products. *Nat. Prod. Rep.* **2023**, *40*, 275–325. [[CrossRef](#)] [[PubMed](#)]
2. Carroll, A.R.; Copp, B.R.; Davis, R.A.; Keyzers, R.A.; Prinsep, M.R. Marine natural products. *Nat. Prod. Rep.* **2021**, *38*, 362–413. [[CrossRef](#)] [[PubMed](#)]
3. Carroll, A.R.; Copp, B.R.; Davis, R.A.; Keyzers, R.A.; Prinsep, M.R. Marine natural products. *Nat. Prod. Rep.* **2022**, *39*, 1122–1171. [[CrossRef](#)] [[PubMed](#)]
4. Zain Ul Arifeen, M.; Ma, Y.N.; Xue, Y.R.; Liu, C.H. Deep-sea fungi could be the new arsenal for bioactive molecules. *Mar. Drugs* **2019**, *18*, 9. [[CrossRef](#)] [[PubMed](#)]
5. Sun, C.; Mudassir, S.; Zhang, Z.; Feng, Y.; Chang, Y.; Che, Q.; Gu, Q.; Zhu, T.; Zhang, G.; Li, D. Secondary metabolites from deep-sea derived microorganisms. *Curr. Med. Chem.* **2020**, *27*, 6244–6273. [[CrossRef](#)] [[PubMed](#)]
6. Skropeta, D.; Wei, L. Recent advances in deep-sea natural products. *Nat. Prod. Rep.* **2014**, *31*, 999–1025. [[CrossRef](#)] [[PubMed](#)]
7. Skropeta, D. Deep-sea natural products. *Nat. Prod. Rep.* **2008**, *25*, 1131–1166. [[CrossRef](#)]
8. Hu, X.; Li, X.; Yang, S.; Li, X.; Wang, B.; Meng, L. Vercytochalasins A and B: Two unprecedented biosynthetically related cytochalasins from the deep-sea-sourced endozoic fungus *Curvularia verruculosa*. *Chin. Chem. Lett.* **2023**, *34*, 107516. [[CrossRef](#)]

9. Yan, L.H.; Li, P.H.; Li, X.M.; Yang, S.Q.; Liu, K.C.; Wang, B.G.; Li, X. Chevalinulins A and B, proangiogenic alkaloids with a spiro[bicyclo[2.2.2]octane-diketopiperazine] skeleton from deep-sea cold-seep-derived fungus *Aspergillus chevalieri* CS-122. *Org. Lett.* **2022**, *24*, 2684–2688. [[CrossRef](#)]
10. Liu, F.A.; Lin, X.; Zhou, X.; Chen, M.; Huang, X.; Yang, B.; Tao, H. Xanthonones and quinolones derivatives produced by the deep-sea-derived fungus *Penicillium* sp. SCSIO Ind16F01. *Molecules* **2017**, *22*, 1999. [[CrossRef](#)]
11. Isaka, M.; Palasarn, S.; Kocharin, K.; Saenboonrueng, J. A cytotoxic xanthone dimer from the entomopathogenic fungus *Aschersonia* sp. BCC 8401. *J. Nat. Prod.* **2005**, *68*, 945–946. [[CrossRef](#)] [[PubMed](#)]
12. Lee, Y.M.; Li, H.; Hong, J.; Cho, H.Y.; Bae, K.S.; Kim, M.A.; Kim, D.K.; Jung, J.H. Bioactive metabolites from the sponge-derived fungus *Aspergillus versicolor*. *Arch. Pharm. Res.* **2010**, *33*, 231–235. [[CrossRef](#)] [[PubMed](#)]
13. Fredimoses, M.; Zhou, X.; Ai, W.; Tian, X.; Yang, B.; Lin, X.; Liu, J.; Liu, Y. Emerixanthone E, a new xanthone derivative from deep sea fungus *Emericella* sp. SCSIO 05240. *Nat. Prod. Res.* **2019**, *33*, 2088–2094. [[CrossRef](#)] [[PubMed](#)]
14. Ma, T.T.; Shan, W.G.; Ying, Y.M.; Ma, L.F.; Liu, W.H.; Zhan, Z.J. Xanthonones with  $\alpha$ -glucosidase inhibitory activities from *Aspergillus versicolor*, a fungal endophyte of *Huperzia serrata*. *Helv. Chim. Acta* **2015**, *98*, 148–152. [[CrossRef](#)]
15. Lesch, B.; Brase, S. A short, atom-economical entry to tetrahydroxanthenones. *Angew. Chem. Int. Ed. Engl.* **2004**, *43*, 115–118. [[CrossRef](#)]
16. Masters, K.S.; Brase, S. Xanthonones from fungi, lichens, and bacteria: The natural products and their synthesis. *Chem. Rev.* **2012**, *112*, 3717–3776. [[CrossRef](#)]
17. Verissimo, A.C.S.; Pinto, D.; Silva, A.M.S. Marine-derived xanthone from 2010 to 2021: Isolation, bioactivities and total synthesis. *Mar. Drugs* **2022**, *20*, 347. [[CrossRef](#)]
18. Niu, S.; Xie, C.L.; Xia, J.M.; Liu, Q.M.; Peng, G.; Liu, G.M.; Yang, X.W. Botryotins A–H, tetracyclic diterpenoids representing three carbon skeletons from a deep-sea-derived *Botryotinia fuckeliana*. *Org. Lett.* **2020**, *22*, 580–583. [[CrossRef](#)]
19. Xie, C.L.; Liu, Q.; He, Z.H.; Gai, Y.B.; Zou, Z.B.; Shao, Z.Z.; Liu, G.M.; Chen, H.F.; Yang, X.W. Discovery of andrastones from the deep-sea-derived *Penicillium allii-sativi* MCCC 3A00580 by OSMAC strategy. *Bioorg. Chem.* **2021**, *108*, 104671. [[CrossRef](#)]
20. Xie, C.L.; Zhang, D.; Guo, K.Q.; Yan, Q.X.; Zou, Z.B.; He, Z.H.; Wu, Z.; Zhang, X.K.; Chen, H.F.; Yang, X.W. Meroterpenothiazole A, a unique meroterpenoid from the deep-sea-derived *Penicillium allii-sativi*, significantly inhibited retinoid X receptor (RXR)- $\alpha$  transcriptional effect. *Chin. Chem. Lett.* **2022**, *33*, 2057–2059. [[CrossRef](#)]
21. He, Z.H.; Xie, C.L.; Wu, T.; Yue, Y.T.; Wang, C.F.; Xu, L.; Xie, M.M.; Zhang, Y.; Hao, Y.J.; Xu, R.; et al. Tetracyclic steroids bearing a bicyclo[4.4.1] ring system as potent antiosteoporosis agents from the deep-sea-derived fungus *Rhizopus* sp. W23. *J. Nat. Prod.* **2023**, *86*, 157–165. [[CrossRef](#)] [[PubMed](#)]
22. Trisuwan, K.; Rukachaisirikul, V.; Kaewpet, M.; Phongpaichit, S.; Hutadilok-Towatana, N.; Preedanon, S.; Sakayaroj, J. Sesquiterpene and xanthone derivatives from the sea fan-derived fungus *Aspergillus sydowii* PSU-F154. *J. Nat. Prod.* **2011**, *74*, 1663–1667. [[CrossRef](#)] [[PubMed](#)]
23. Holker, J.S.E.; O'Brien, E.; Simpson, T.J. The structures of some metabolites of *Penicillium diversum*:  $\alpha$ - and  $\beta$ -diversonolic esters. *J. Chem. Soc. Perkin Trans. 1* **1983**, 1365–1368. [[CrossRef](#)]
24. Nicolaou, K.C.; Li, A. Total syntheses and structural revision of  $\alpha$ - and  $\beta$ -diversonolic esters and total syntheses of diversonol and blennolide C. *Angew. Chem. Int. Ed. Engl.* **2008**, *47*, 6579–6582. [[CrossRef](#)] [[PubMed](#)]
25. Shao, C.; Wang, C.; Wei, M.; Gu, Y.; Xia, X.; She, Z.; Lin, Y. Structure elucidation of two new xanthone derivatives from the marine fungus *Penicillium* sp. (ZZF 32#) from the south china sea. *Magn. Reson. Chem.* **2008**, *46*, 1066–1069. [[PubMed](#)]
26. Sun, R.R.; Miao, F.P.; Zhang, J.; Wang, G.; Yin, X.L.; Ji, N.Y. Three new xanthone derivatives from an algicolous isolate of *Aspergillus wentii*. *Magn. Reson. Chem.* **2013**, *51*, 65–68. [[CrossRef](#)]
27. Cui, X.; Zhu, G.; Liu, H.; Jiang, G.; Wang, Y.; Zhu, W. Diversity and function of the antarctic krill microorganisms from *Euphausia superba*. *Sci. Rep.* **2016**, *6*, 36496. [[CrossRef](#)]
28. Hamasaki, T.; Sato, Y.; Hatsuda, Y. Structure of sydowinin A, sydowinin B, and sydowinol, metabolites from *Aspergillus sydowii*. *Agric. Biol. Chem.* **2014**, *39*, 2341–2345. [[CrossRef](#)]
29. Song, X.Q.; Zhang, X.; Han, Q.J.; Li, X.B.; Li, G.; Li, R.J.; Jiao, Y.; Zhou, J.C.; Lou, H.X. Xanthone derivatives from *Aspergillus sydowii*, an endophytic fungus from the liverwort *Scapania ciliata* S. Lac and their immunosuppressive activities. *Phytochem. Lett.* **2013**, *6*, 318–321. [[CrossRef](#)]
30. Zhu, F.; Lin, Y.C. Three xanthonones from a marine-derived mangrove endophytic fungus. *Chem. Nat. Compd.* **2007**, *43*, 132–135. [[CrossRef](#)]
31. Shao, C.; She, Z.; Guo, Z.; Peng, H.; Cai, X.; Zhou, S.; Gu, Y.; Lin, Y. <sup>1</sup>H and <sup>13</sup>C NMR assignments for two anthraquinones and two xanthonones from the mangrove fungus (ZSUH-36). *Magn. Reson. Chem.* **2007**, *45*, 434–438. [[CrossRef](#)] [[PubMed](#)]
32. Graybill, T.L.; Casillas, E.G.; Pal, K.; Townsend, C.A. Silyl triflate-mediated ring-closure and rearrangement in the synthesis of potential bisfuran-containing intermediates of aflatoxin biosynthesis. *J. Am. Chem. Soc.* **1999**, *121*, 7729–7746. [[CrossRef](#)]
33. Dou, Y.; Wang, X.; Jiang, D.; Wang, H.; Jiao, Y.; Lou, H.; Wang, X. Metabolites from *Aspergillus versicolor*, an endolichenic fungus from the lichen *Lobaria retigera*. *Drug Discov. Ther.* **2014**, *8*, 84–88. [[CrossRef](#)] [[PubMed](#)]
34. Liu, X.B.; Zheng, N.; Liang, L.Q.; Zhao, D.M.; Qin, Y.Y.; Li, J.; Yang, R.Y. Secondary metabolites from the endophytic fungus *Fusarium equiseti* and their antibacterial activities. *Chem. Nat. Compd.* **2019**, *55*, 1141–1144. [[CrossRef](#)]
35. Yamazaki, M.; Satoh, Y.; Maebayashi, Y.; Horie, Y. Monoamine oxidase inhibitors from a fungus, *Emericella navahoensis*. *Chem. Pharm. Bull.* **1988**, *36*, 670–675. [[CrossRef](#)]

36. Steyn, P.S.; Vlegaar, R.; Wessels, P.L.; Cole, R.J.; Scott, D.B. Structure and carbon-13 nuclear magnetic resonance assignments of versiconal acetate, versiconol acetate, and versiconol, metabolites from cultures of *Aspergillus parasiticus* treated with dichlorvos. *J. Chem. Soc. Perkin Trans. 1* **1979**, 451–459. [[CrossRef](#)]
37. Liu, D.; Yan, L.; Ma, L.; Huang, Y.; Pan, X.; Liu, W.; Lv, Z. Diphenyl derivatives from coastal saline soil fungus *Aspergillus izuzakae*. *Arch. Pharm. Res.* **2015**, *38*, 1038–1043. [[CrossRef](#)]
38. Lu, Z.; Zhu, H.; Fu, P.; Wang, Y.; Zhang, Z.; Lin, H.; Liu, P.; Zhuang, Y.; Hong, K.; Zhu, W. Cytotoxic polyphenols from the marine-derived fungus *Penicillium expansum*. *J. Nat. Prod.* **2010**, *73*, 911–914. [[CrossRef](#)]
39. Li, X.B.; Zhou, Y.H.; Zhu, R.X.; Chang, W.Q.; Yuan, H.Q.; Gao, W.; Zhang, L.L.; Zhao, Z.T.; Lou, H.X. Identification and biological evaluation of secondary metabolites from the endolichenic fungus *Aspergillus versicolor*. *Chem. Biodivers.* **2015**, *12*, 575–592. [[CrossRef](#)]
40. Sanchez, J.F.; Chiang, Y.M.; Szewczyk, E.; Davidson, A.D.; Ahuja, M.; Elizabeth Oakley, C.; Woo Bok, J.; Keller, N.; Oakley, B.R.; Wang, C.C. Molecular genetic analysis of the orsellinic acid/F9775 gene cluster of *Aspergillus nidulans*. *Mol. Biosyst.* **2010**, *6*, 587–593. [[CrossRef](#)] [[PubMed](#)]
41. Wei, P.Y.; Li, L.; Yang, C.G.; Luo, D.Q.; Zheng, Z.H.; Lu, X.H.; Shi, B.Z. A novel oxybis cresol verticilatin with highly varying degrees of biological activities from the insect pathogenic fungus *Paecilomyces verticillatus*. *J. Asian Nat. Prod. Res.* **2014**, *16*, 1153–1157. [[CrossRef](#)]
42. Hu, S.S.; Jiang, N.; Wang, X.L.; Chen, C.J.; Fan, J.Y.; Wurin, G.G.; Ge, H.M.; Tan, R.X.; Jiao, R.H. Prenylated diphenyl ethers from the mantis-associated fungus *Aspergillus versicolor* GH-2. *Tetrahedron Lett.* **2015**, *56*, 3894–3897. [[CrossRef](#)]
43. Wang, X.; Mou, Y.; Hu, J.; Wang, N.; Zhao, L.; Liu, L.; Wang, S.; Meng, D. Cytotoxic polyphenols from a sponge-associated fungus *Aspergillus versicolor* Hmp-48. *Chem. Biodivers.* **2014**, *11*, 133–139. [[CrossRef](#)]
44. Eamvijarn, A.; Kijjoa, A.; Bruyere, C.; Mathieu, V.; Manoch, L.; Lefranc, F.; Silva, A.; Kiss, R.; Herz, W. Secondary metabolites from a culture of the fungus *Neosartorya pseudofischeri* and their in vitro cytostatic activity in human cancer cells. *Planta Med.* **2012**, *78*, 1767–1776. [[CrossRef](#)] [[PubMed](#)]
45. Grundmann, A.; Li, S.M. Overproduction, purification and characterization of FtmPT1, a brevianamide F prenyltransferase from *Aspergillus fumigatus*. *Microbiology* **2005**, *151*, 2199–2207. [[CrossRef](#)]
46. Tsukamoto, S.; Kato, H.; Samizo, M.; Nojiri, Y.; Onuki, H.; Hirota, H.; Ohta, T. Notoamides F-K, prenylated indole alkaloids isolated from a marine-derived *Aspergillus* sp. *J. Nat. Prod.* **2008**, *71*, 2064–2407. [[CrossRef](#)] [[PubMed](#)]
47. Kato, H.; Yoshida, T.; Tokue, T.; Nojiri, Y.; Hirota, H.; Ohta, T.; Williams, R.M.; Tsukamoto, S. Notoamides A–D: Prenylated indole alkaloids isolated from a marine-derived fungus, *Aspergillus* sp. *Angew. Chem. Int. Ed. Engl.* **2007**, *46*, 2254–2256. [[CrossRef](#)] [[PubMed](#)]
48. Peng, J.; Gao, H.; Zhang, X.; Wang, S.; Wu, C.; Gu, Q.; Guo, P.; Zhu, T.; Li, D. Psychrophilins E-H and versicotide C, cyclic peptides from the marine-derived fungus *Aspergillus versicolor* ZLN-60. *J. Nat. Prod.* **2014**, *77*, 2218–2223. [[CrossRef](#)]
49. Kobori, M.; Yoshida, M.; Ohnishi-Kameyama, M.; Takei, T.; Shinmoto, H. 5 $\alpha$ ,8 $\alpha$ -Epidioxy-22E-ergosta-6,9(11),22-trien-3 $\beta$ -ol from an edible mushroom suppresses growth of HL60 leukemia and HT29 colon adenocarcinoma cells. *Biol. Pharm. Bull.* **2006**, *29*, 755–759. [[CrossRef](#)]
50. Dixon, S.J.; Lemberg, K.M.; Lamprecht, M.R.; Skouta, R.; Zaitsev, E.M.; Gleason, C.E.; Patel, D.N.; Bauer, A.J.; Cantley, A.M.; Yang, W.S.; et al. Ferroptosis: An iron-dependent form of nonapoptotic cell death. *Cell* **2012**, *149*, 1060–1072. [[CrossRef](#)]
51. Gao, M.; Monian, P.; Pan, Q.; Zhang, W.; Xiang, J.; Jiang, X. Ferroptosis is an autophagic cell death process. *Cell Res.* **2016**, *26*, 1021–1032. [[CrossRef](#)] [[PubMed](#)]
52. Hofmans, S.; Vanden Berghe, T.; Devisscher, L.; Hassannia, B.; Lyssens, S.; Joossens, J.; Van Der Veken, P.; Vandenabeele, P.; Augustyns, K. Novel ferroptosis inhibitors with improved potency and ADME properties. *J. Med. Chem.* **2016**, *59*, 2041–2053. [[CrossRef](#)] [[PubMed](#)]
53. Stockwell, B.R. Ferroptosis turns 10: Emerging mechanisms, physiological functions, and therapeutic applications. *Cell* **2022**, *185*, 2401–2421. [[CrossRef](#)]
54. Feng, H.; Li, F.; Tang, P. Circ\_0000745 regulates NOTCH1-mediated cell proliferation and apoptosis in pediatric T-cell acute lymphoblastic leukemia through adsorbing miR-193b-3p. *Hematology* **2021**, *26*, 885–895. [[CrossRef](#)] [[PubMed](#)]
55. Peng, X.; Tan, Q.; Wu, L.; Wu, D.; Xu, J.; Zhou, H.; Gu, Q. Ferroptosis Inhibitory aromatic abietane diterpenoids from *Ajuga decumbens* and structural revision of two 3,4-epoxy group-containing abietanes. *J. Nat. Prod.* **2022**, *85*, 1808–1815. [[CrossRef](#)] [[PubMed](#)]

**Disclaimer/Publisher’s Note:** The statements, opinions and data contained in all publications are solely those of the individual author(s) and contributor(s) and not of MDPI and/or the editor(s). MDPI and/or the editor(s) disclaim responsibility for any injury to people or property resulting from any ideas, methods, instructions or products referred to in the content.